Korean Journal of Remote Sensing, Vol.23, No.3, 2007, pp.211~219

A Semi-automated Method to Extract 3D Building Structure

Tsend-Ayush Javzandulam*, Taejung Kim* †, and Kyung-Ok Kim**

* Department of Geoinformatic Engineering, Inha University

** Spatial Information Research Team, Electronics and Telecommunications Research Institute

Abstract : Building extraction is one of the essential issues for 3D city modelling. In recent years, high-resolution satellite imagery has become widely available and it brings new methodology for urban mapping. In this paper, we have developed a semi-automatic algorithm to determine building heights from monoscopic high-resolution satellite data. The algorithm is based on the analysis of the projected shadow and actual shadow of a building. Once two roof corner points are measured manually, the algorithm detects (rectangular) roof boundary automatically. Then it estimates a building height automatically by projecting building shadow onto the image for a given building height, counting overlapping pixels between the projected shadow and actual shadow, and finding the height that maximizes the number of overlapping pixels. Once the height and roof boundary are available, the footprint and a 3D wireframe model of a building can be determined. The proposed algorithm is tested with IKONOS images over Deajeon city and the result is compared with the building height determined by stereo analysis. The accuracy of building height extraction is examined using standard error of estimate.

Key Words : feature extraction, shadow analysis, high-resolution image.

1. Introduction

3D city modelling has become increasingly interested for recent several years because of its significant role in many application areas, such as in communication industry, urban microclimate and pollution control analysis, transportation navigation, landscape planning and visualization, etc. One of the essential issues for 3D city modelling is building extraction. Most of the previous approaches on building extraction used light detection and ranging (LIDAR) and stereo analysis. Recently, high-resolution satellite imagery has become available and they give an opportunity of mapping urban details.

Ridley *et al.* (1997) evaluated the potential of 1-m resolution satellite imagery for building extraction and reported that only 73% and 86% of buildings could be interpreted correctly using monoscopic and stereoscopic imagery, respectively. Sohn and Dowman (2001) reported an investigation on building extraction from high-resolution imagery. However, the study dealt only with large detached buildings and a comprehensive analysis of accuracy and completeness in modelling structural details was

Received 6 May 2007; Accepted 19 June 2007.

† Corresponding Author: Taejung Kim (tezid@inha.ac.kr)

not performed.

Many researchers have been trying to extract 3D objects automatically. Most of them used airborne and spaceborne data (Kim and Muller, 1996; Baltsavias *et al.*, 1997; Haala and Brenner, 1999; G?lch *et al.*, 1999; Farhad *et al.*, 2005;) and some used high resolution stereo images. (Kim and Muller,1998; Kim *et al.* 2006). Until now, fully automatic feature extraction systems are limited only to specific applications. However, in recent years, high spatial resolution satellite images provide a new data source for building extraction. They have several advantages including the cost and the accessibility. In order to effectively utilize the potential of high-resolution satellite imagery for building extraction, new methods and tools are required.

The objective of this research is to develop an algorithm to extract 3D buildings from monoscopic high-resolution satellite images. The proposed algorithm is initiated by manually selected two roof corner points of a building. With these two points, the algorithm extracts building lines using monoscopic line analysis (Kim *et al.*, 2006) and detects roof boundary. Then it estimates a building height automatically. Once the building height is available, the footprint and a 3D wireframe model of a building can be determined. In this study we assume that buildings have a flat roof of a uniform height on the top of rectangular solids. Walls are considered to be vertical and each building casts its shadow on a surface that is locally flat.

2. Algorithm Description

The algorithm flow is described in Fig. 1. Firstly, we provide any two opposite roof corner points of a building. Using those corner points we can define a region of interest (ROI). Then, we extract building

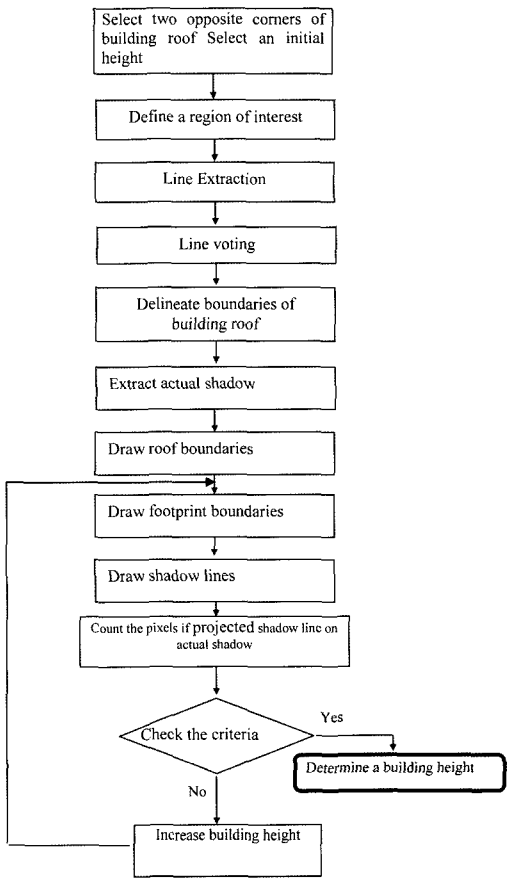

Fig. 1. Workflow of the building height extraction algorithm.

lines within the defined ROI and a line voting process is applied to estimate the orientation of a building roof line. There is a similar estimation method using line voting and matching (Kim *et al.*, 2004; Kim *et al.*, 2006). Next, we delineate the whole boundary of a building roof. Once the building roof boundary is delineated, we can draw the shadow of a building. The direction of shadow lines and vertical lines of a building within a satellite image can be determined by the azimuth and elevation angles of the sun and the satellite. We change building heights incrementally, calculate the extent of a shadow region for each height and project the building shadow onto the image. Then, we count overlapping pixels between the projected shadow and actual shadow,

which is extracted by a simple thresholding. We determine the height that maximizes the number of overlapping pixels as the height of a building. Once we know the building height and the roof boundary, we can determine the boundary of building footprint by shifting the roof boundary along the direction of vertical lines by the amount of the building height. Then, the roof, footprints and vertical lines can constitute a 3D wireframe model of a building.

1) Defining a region of interest

We first select any two opposite roof corner points, $R_1(x_1, y_1)$ and $R_2(x_2, y_2)$, of a building manually. Then, we define a ROI to include the area covered by all potential buildings that can be defined by the selected two corners. We consider that buildings are rectangular shaped. We can extract the ROI based on the following consideration. If $R_1(x_1, y_1)$ and $R_2(x_2, y_2)$ are two opposite points of a building roof, the other two unknown corner points, $R_3(x_3, y_3)$ and $R_4(x_4, y_4)$, are then on the circle with the diameter of $|R_1(x_1, y_1)\ R_2(x_2, y_2)|$. $R_3(x_3, y_3)$ and $R_4(x_4, y_4)$ points are symmetric points for diameter and the coordinates of the points should be within $[AO]$, $[CO]$ and $[O\ A']$, $[O\ C']$ intervals respectively (Fig. 2).

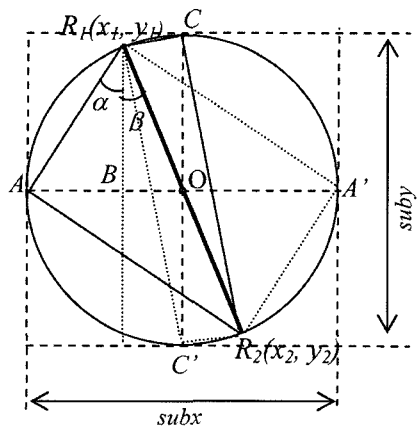

Fig. 2. Definition of a region of interest.

$$R_3(x_3, y_3): \begin{cases} x_3 \in [A;O] \\ y_3 \in [C;O] \end{cases} \quad (1)$$

$$R_4(x_4, y_4): \begin{cases} x_4 \in [O;A'] \\ y_4 \in [O;C'] \end{cases} \quad (2)$$

where,

$$O(ox, oy): ox = x_1 + \frac{1}{2}\sqrt{(x_1 - x_1)^2} \quad oy = y_1 + \frac{1}{2}\sqrt{(y_1 - y_1)^2}$$

$$A(ax, ay): ax = x_1 - \frac{1}{2}\sqrt{(x_1 - x_2)^2 + (y_1 - y_2)^2}\,(1 - \sin\beta)$$
$$ay = ox$$

$$A'(ax', ay'): ax' = x_2 + \frac{1}{2}\sqrt{(x_1 - x_2)^2 + (y_1 - y_2)^2}\,(1 - \sin\beta)$$
$$ay' = oy$$

$$C(cx, cy): cx = ox \quad cy = y_1 - \frac{1}{2}\sqrt{(x_1 - x_2)^2 + (y_1 - y_2)^2}$$
$$(1 - \cos\beta)$$

$$C'(cx', cy'): cx' = ox \quad cy' = y_2 - \frac{1}{2}\sqrt{(x_1 - x_2)^2 + (y_1 - y_2)^2}$$
$$(1 - \cos\beta)$$

$$\beta = \arctan\left(\frac{|x_1 - x_2|}{|y_1 - y_2|}\right)$$

Therefore ROI = $ROI(subx, suby)$ is defined as follows:

$$subx = [ax;ax'] \quad suby = [cy;cy'] \quad (5)$$

2) Estimating a roof boundary

After defining a ROI, we extract lines by applying the line extraction algorithm proposed by Burns *et al* (1986). This algorithm defines "line-support regions" by grouping pixels with similar edge orientation and magnitude together and extracts a line from each line support region by planar fitting. After line extraction we vote the lines to find the orientation of the longer side of a building of interest. The geometry of two roof corners, $R_1(x_1, y_1)$ and $R_2(x_2, y_2)$, shows that a longer sideline of a building must lie within the angular segment between γ and $\gamma + 90°$ angles (Fig. 3). For voting, we divide the angular segment into smaller bins by drawing lines from the corner point $R_1(x_1, y_1)$ with an angular increment $\Delta\gamma$. Here,

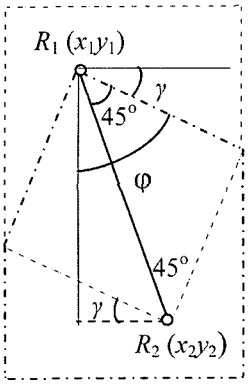

Fig. 3. Segments of longer sides of a building.

$$\gamma = 90^\circ - \arctan\left(\frac{|y_1 - y_2|}{|x_1 - x_2|}\right) \quad (3)$$

$$\Delta\gamma = 90^\circ - \frac{90^\circ(L-\varepsilon)}{L} \quad (4)$$

where,

$$L = |y_1 - y_2| * \left(\tan(\varphi) + \frac{1}{\tan(\varphi)}\right)$$

$$\varphi = 45^\circ - \arctan\left(\frac{|y_1 - y_2|}{|x_1 - x_2|}\right)$$

ε- small number

Simultaneously, we divide the segment by drawing lines from corner point $R_2(x_2, y_2)$ with the same angle increment $\Delta\gamma$. For each angular bin, we count the number of extracted line elements. Then we select the bin with the maximum line elements. Since the bin selected will contain more line elements than any other bins, this bin will most probably be the one for the longer side of a building roof. After defining the building orientation ϕ, the unknown roof corners, $R_3(x_3, y_3)$ and $R_4(x_4, y_4)$, can be defined as follows:

$$\begin{cases} x_{3,4} = x_{1,2} \pm \sqrt{(x_1 - x_2)^2 + (y_1 - y_2)^2}\sin\xi\sin\phi\, sign(\cos(\phi)) \\ x_{3,4} = x_{1,2} \mp \sqrt{(x_1 - x_2)^2 + (y_1 - y_2)^2}\sin\xi\sin\phi\, sign(\cos(\phi)) \end{cases} \quad (6)$$

where,

$$\xi = \begin{cases} \arctan\left(\frac{|x_1 - x_2|}{|y_1 - y_2|}\right) + \phi - 90^0, & \phi \le 90^0 \\ \arctan\left(\frac{|x_1 - x_2|}{|y_1 - y_2|}\right) - \phi + 90^0, & \phi > 90^0 \end{cases}$$

Since the four roof corner points are defined, we can delineate the whole boundary of a building.

3) Estimating a building height

The directions of a building vertical line and building shadow are indicated by the azimuth angle and elevation angle of the satellite and the sun. The length of a vertical line and shadow line for a given height can be determined by the elevation angle of the satellite and the sun. Lee and Kim (2005) determined building heights interactively by projecting a shadow region for a given building height onto the image and by adjusting the height manually until the projected shadow and actual shadow match. In this paper, we aim to determine building heights automatically.

The initial height of a building is selected as h=1 pixel. Since the roof boundary and height are known, the corner points of the building footprint, (px_i^h, py_i^h), $i = 1,2,\cdots, BL$, can be defined as follows:

$$\begin{cases} px_i^h = rx_i^o + \Delta x_v \\ py_i^h = ry_i^o + \Delta y_v \end{cases} \quad i = 1,2,\cdots, BL$$

$$\Delta y_v = \frac{h}{\tan(El)} \times \sin(Az) \quad (7)$$

$$\Delta x_v = \frac{h}{\tan(El)} \times \cos(Az)$$

where (rx_i^o, ry_i^o) are the corner points of the building roof, h is the building height, Az and El are the azimuth angle and elevation angles of the satellite, respectively.

After determining the footprint boundary, the points of the shadow lines (sx_i^h, sy_i^h) $i = 1,2,\cdots, BL$ can be defined as follows,

$$\begin{cases} sx_i^h = px_i^h + \Delta x_s \\ sy_i^h = py_i^h + \Delta y_s \end{cases} \quad i = 1,2,\cdots, BL$$

$$\Delta x_s = \frac{h}{\tan(SEl)} \times \cos(SAz) \qquad (8)$$

$$\Delta y_s = \frac{h}{\tan(SEl)} \times \sin(SAz)$$

where SAz and SEl are the azimuth and elevation angles of the sun, respectively. We then draw shadow lines as we increase the building height by one pixel. For every step, we count the number of the points of the projected shadow lines that lie within the actual shadow region. Let us denote the number of the counted points at the h^{th} height as PN^h. Then this process continues until PN^h reaches zero.

$$PN^h = \sum_{i=1}^{BL} Temp_i$$

$$Temp_i = \begin{cases} \sum_{i=1}^{BL} k \;\; if \;\; \forall k : (sx_{i_k}^h, sy_{i_k}^h) \in AS \\ 0 \quad otherwise \end{cases} \qquad (9)$$

$$SL = \frac{h}{\tan(SEl)}$$

SL is the length of a projected shadow line and AS is the actual shadow region. The building height is accepted as H, which maximizes the value of PN.

$$H : PN^H = \max_h PN^h \qquad (10)$$

Fig. 4 shows the diagram of the roof, footprint and shadow lines of a building. Once we determine the building height, we can obtain the coordinates of the corners of a building footprint (Eq. 7).

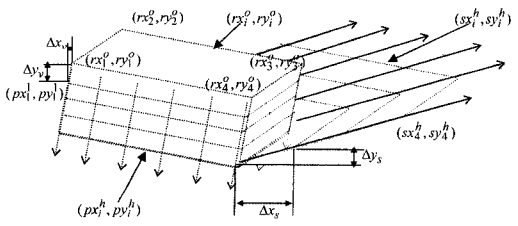

Fig. 4. Diagram of roof, footprint and shadow lines.

3. Results and Performance

An IKONOS image over Daejeon city of Korea was used to assess the performance of the proposed algorithm. The image contains a lot of residential and industrial buildings with various sizes and shapes. It is shown in Fig. 5. We defined seven sub-regions in the image that contain rectangular-shaped buildings of large size. We extracted building roof boundaries with different increment angle (Eq. 4). Firstly, employing the algorithm with ε=1, we extracted 62 building roof lines from the defined seven sub-regions. Fig. 6 shows some examples of extracted

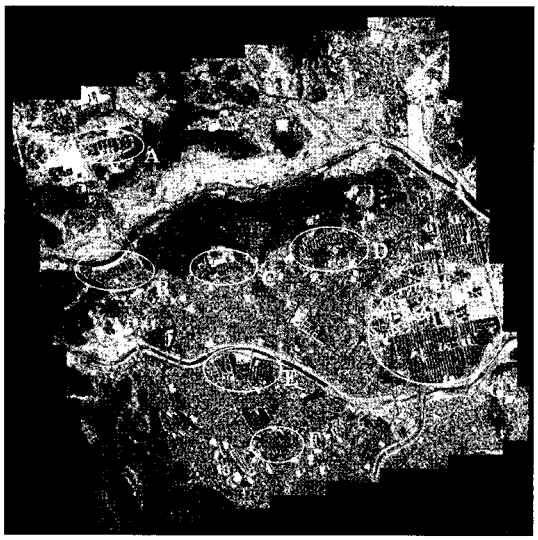

Fig. 5. An IKONOS image over Daejeon. The circles indicate the sub-regions.

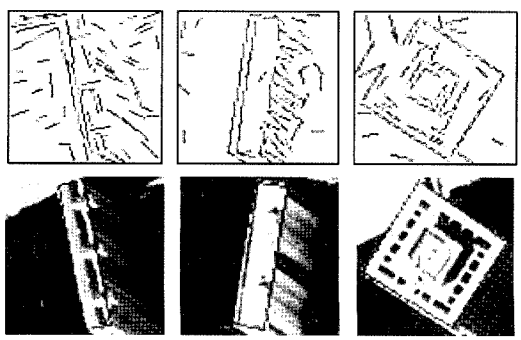

Fig. 6. Line images (upper), Roof boundaries (lower).

line images and roof boundaries. To verify the proposed algorithm, we measured the building orientation manually for the same 62 buildings and the results were compared. The summarized results of building roof extraction per each sub-region are shown in Table 1. The second column of Table 1 shows the number of buildings tested within each sub-region, the third and fourth column the angular differences between extracted lines and true building lines in angle and in pixel, respectively. The average angular error of the total extracted building roofs was 1.71 degrees or 0.56 pixels.

Table 1. Assessment of building roof extraction.

Sub-region ID	No of extracted building	Angular error (degrees)	Angular error (pixels)
A	6	1.50	1.22
B	11	1.63	0.54
C	6	1.00	0.44
D	5	0.80	0.34
E	14	1.35	0.61
F	9	0.77	0.36
G	11	1.90	0.90
Average	62	1.71	0.56

We tested the algorithm with different increment angles such as ε=2, 4, 6 and extracted 12 building roof lines for each case. The examples of the extracted roof lines for each increment angle are shown in Fig. 7 and the results of accuracy assessment with each increment angle are shown in Table 2. The average angular error was 1.74 degrees in case of ε=2, 2.94 in case of ε=4 and 4.21 in case of ε=6. The results showed that the accuracy could be improved by reducing the increment angle.

After building roof extraction, we tested automatic height extraction against 30 buildings. Since the proposed algorithm is based on shadow analysis, we tested the height extraction only when the actual shadow of a building was visible and not blocked. Fig.

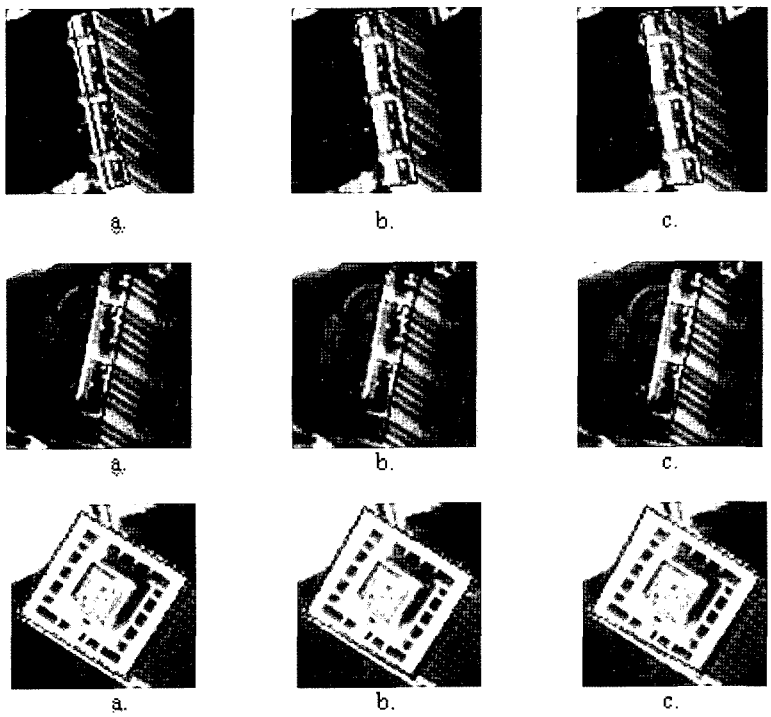

Fig. 7. Examples of building line extraction. (a) ε=2, (b) ε=4, (c) ε=6.

Table 2. Results of assessment of building roof extraction in case of ε = 2, 4, and 6.

Building ID	ε=2 (degrees)	ε=4 (degrees)	ε=6 (degrees)
AA1	2.77	2.77	3.47
AA2	2.99	4.49	5.97
AA3	3.24	4.05	4.86
BB1	0.79	1.57	3.27
BB2	0.83	2.48	3.46
BB3	0.00	1.13	3.67
EE1	0.00	2.81	7.43
EE2	2.42	3.22	2.42
EE3	0.73	1.47	3.73
GG1	0.71	1.42	1.42
GG2	4.18	5.84	6.05
GG3	1.41	4.10	5.46
Average	1.74	2.94	4.21

8 shows some examples of building height extraction. The upper part of the figure shows the original buildings and the lower part 3D wireframe models of the buildings with their projected shadow regions.

To estimate the accuracy of building height extraction, we measured building height manually using an IKONOS stereo pair. A building height was calculated by measuring tie points on a building roof and tie points on the ground and by calculating the height difference of the two tie points. We assumed that the building height obtained by stereo analysis was true and the extracted building height was compared with the building height by stereo analysis.

Table 3. Assessment of building height extraction.

Sub-region ID	No of extracted building	Difference error between extracted and measured building height (m)
A	5	1.51
B	4	0.62
C	3	0.33
D	3	0.98
E	2	0.60
F	3	1.12
G	10	1.69
Average	30	1.86

The differences are shown in Table 3. The

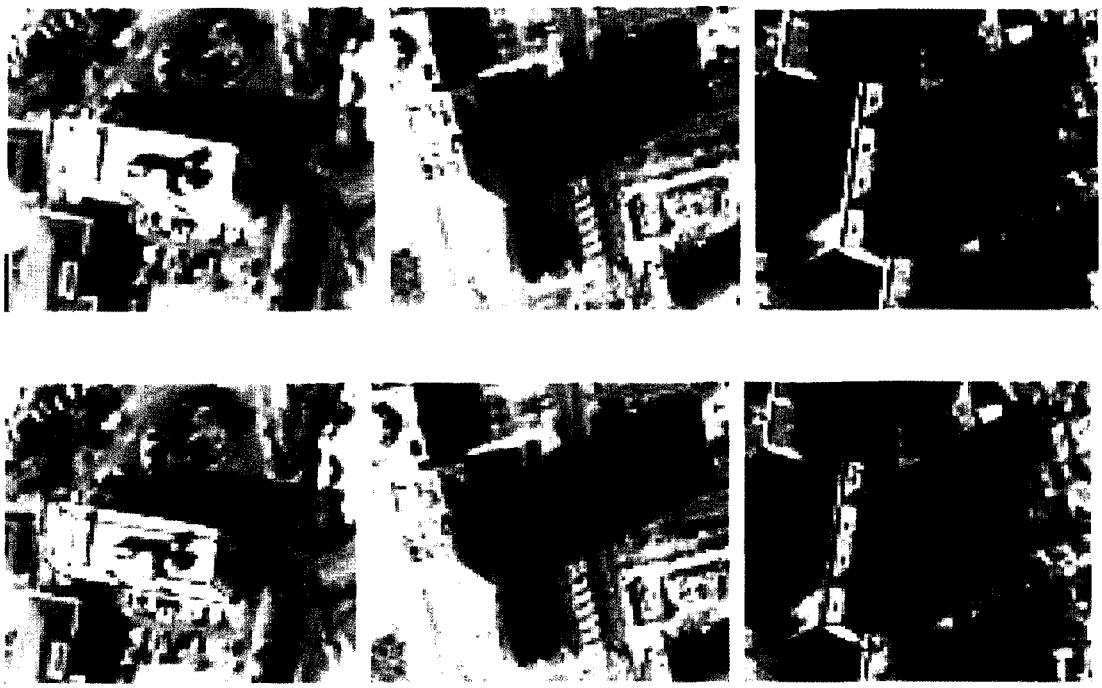

Fig. 8. Examples of the original buildings (upper) and extracted 3D wireframe models and their shadows (lower).

accuracy of the building height extraction was examined using the standard error of estimate and it was found that standard error was 1.86 m.

4. Conclusions

A new approach for semi-automatic building height extraction based on building shadow analysis of the projected shadow and actual shadow is presented in this paper. The satellite scene geometry and building roof corner points are used as inputs to the proposed algorithm. The proposed algorithm contains two parts. The first part delineates whole building boundary using any of two opposite roof corner points. Assuming roofs of rectangular shapes, we extract longer sidelines of a building through a line voting process. The proposed algorithm gives good results if roof boundaries produce strong line elements and the result could be improved by reducing an increment angle. The second part extracts a building height and a 3D wireframe model automatically using the delineated building boundaries. The procedure of building height extraction is based on the analysis of overlapping pixels between the projected shadow and actual shadow. In this study, to detect the actual shadow of a building we apply a simple thresholding. We assume that the whole of the shadow of a building is visible and unblocked by other structures and that the building shadow cast onto the locally flat surface. However, this assumption is not always true. This was the main reason of estimation error of the proposed algorithm.

Acknowledgements

The work in this paper has been partially supported by Korea Research Foundation (KRF-2004-003-D00408).

Reference

Burns, J. B., A. R. Hanson, and E. M. Riseman, 1986. Extracting straight lines, *IEEE Trans. Pattern Analysis and Machine Intelligence*, 8: 425-445.

Baltsavias. E, W. Eckstein, E. Gülch, M. Hahn, D. Stallmann, K. Tempfli, and R. Welch, Editors, 3D Reconstruction and Modeling of Topographic Objects, International Archives of Photogrammetry and Remote Sensing vol. 32, Part B3-4W2 (1997).

Farhad, S., A. Ali, H. Michael, and L. Curo, 2005. Automatic 3D object recognition and reconstruction based on neuro-fuzzy modelling ISPRS Journal of Photogrammetry and Remote Sensing, 59(5): 255-277.

Gülch. E., H. Müller, and T. Läbe, 1999. Integration of automatic processes into semi-automatic building extraction, *International Archives of Photogrammetry and Remote Sensing*, 32(Part 3-2W5): 177-186.

Haala. N. and C. Brenner, 1999. Extraction of buildings and trees in urban environments, *ISPRS Journal of Photogrammetry and Remote Sensing*, 54(2-3): 130-137.

Kim. T., S. Park, M. Kim, S. Jeong, and K. Kim, 2004. Semi Automatic Tracking of Road Centerlines From High Resolution Remote Sensing Data, *Photogrammetric Engineering and Remote Sensing*, 70(12): 1417-1422.

Kim. T. and J. Muller, 1996. Automated Urban Building Extraction from High Resolution Stereo Imagery, *Image and Vision Computing*, 14(2): 115-130.

Kim. T. and J. Muller, 1998. A Technique for 3D Building Extraction, *Photogrammetric Engineering and Remote Sensing*, 64(9): 923-930.

Kim. T., T. Lee, and K. Kim, 2006. Semiautomatic Building Line Extraction from Ikonos Image Through Monoscopic Line analysis, *Photogrammetric Engineering and Remote Sensing*, 72(5): 541-549.

Lee, T. and T. Kim, 2005. Reconstruction of 3D building structures from IKONOS images trough monoscopic line and shadow analysis, Processing of Asian Conference on Remote Sensing, 7-11 Nov, Hanoi, Vietnam.

Ridley, H. M, P. M. Atkinson, P. Aplin, J. P. Muller, and I. Dowman, 1997. Evaluating the potential of the forthcoming commercial US high-resolution satellite sensor imagery at the Ordinance Survey, *Photogramm. Eng. Remote Sens*, 63(8): 997-1005.

Sohn, G. and I. Dowman, 2001. Extraction of buildings from high resolution satellite data. In: E. Baltsavias, A. Gruen and L. Van Gool, Editors, Automated Extraction of Man-Made Objects from Aerial and Space Images (III), Balkema Publishers, Lisse, pp. 345-355.